THE UNIVERSITY OF SYDNEY

bushfire&natural HAZARDSCRC

bnhcrc.com.au

NEAR INFRARED SPECTROSCOPY AS A NEW FIRE SEVERITY METRIC

Milestone 3.3.2 Final report on soil carbon and fire severity

Danica Parnell, Tina Bell, Malcolm Possell
The University of Sydney, NSW

Version	Release history	Date
1.0	Initial release of document	15/05/2020

Publisher:
Bushfire and Natural Hazards CRC

May 2020

Citation: Parnell D, Bell T & Possell M (2020) Near infrared spectroscopy as a

new fire severity metric, Bushfire and Natural Hazards CRC, Melbourne.

Cover: Range of residues (char and ash) remaining after prescribed burning in the Blue Mountains. Source: Danica Parnell.

TABLE OF CONTENTS

ABSTRACT

Samples of leaves, twigs and bark representing typical surface fuels from forests and woodlands were systematically heated until combusted under controlled conditions in the laboratory. Change in colour of residue was described using R-conversion of the Munsell colour system and compared to colours generated from near infrared (NIR) scanning. Regardless of the method of heating used, there was very little change in physical properties or colour of residues when heated at low temperatures to 200 °C. Surface fuel samples began to thermally degrade when heated at 300 °C, which was reflected in much darker coloured residues that were mostly uniform in colour for different fuel types when determined from NIR spectroscopy. When surface fuels were combusted at temperatures between 400 and 600 °C, residues were much lighter in colour regardless of the type of fuel burnt. Again, residue colours were more uniform when described using NIR spectroscopy compared to the Munsell colour system, although differences in the consistency of residues (heterogenous production of charred material and ash) were still reflected in variations in shading. In several instances, colours resulting from NIR scans were closer to the actual colour of residues suggesting that it is a more accurate system than colour matching by eye using the Munsell colour system.

This study indicates that there is potential for NIR technology to be used to determine fire severity according to the colour of residue after fire. While the general method of colour matching is not new, the use of NIR spectroscopy can reduce inaccuracies associated with subjective colour matching and poor colour correlation when using some forms of automated colour conversion. As shown, spectroscopic methods such as NIR can also be used to assess chemical changes in fuels during thermal decomposition. This includes quantitative losses of carbon and nitrogen and estimating fire intensity according to the temperature that were required to form a particular residue.

END-USER STATEMENT

Dr Felipe Aires, NSW National Parks and Wildlife Service

Traditional observations of fire severity in the field are done by observing the percentage of leaf consumption by stratum and percentage of leaf scorched to generate an approximate severity metric. These measures are time consuming and subjective and are prone to human error depending on the observer's experience and time of observation post-fire. This study progresses the knowledge and provides a new way to derive a fire severity metric using handheld NIR scanners and the Munsell colour system. This method removes subjectivity associated with colour matching made by the human eye and has the potential to be derived into a novel fire severity metric.

The spectroscopic data suggests that the technique could also be developed to provide insight into chemical properties of the burnt residues and the implications they may have on ecosystem recovery.

The ability to use handheld NIR systems in the field to accurately determine fire severity presents an exciting opportunity for land management agencies. It could lead to new ways of validating satellite fire severity measures and postfire monitoring potentially saving staff time dedicated to those purposes.

1. INTRODUCTION

Fire, regardless of whether it is planned or unplanned, has an influential role in determining how various organisms interact with each other and with their environment (Adey and Loveland, 2007; Keeley, 2008). For a complex understanding of how fire affects ecosystems, the five components of fire regimes – namely, fuel consumption patterns, fire intensity and severity, fire frequency, patch size and seasonality – need to be investigated (Keeley, 2008). Of these, fire severity is a metric that, amongst other things, estimates the impact that fire intensity has on plant communities. It measures the physical change in an area after fire and describes the immediate effects on vegetation, litter and soil (Sousa, 1984). These variables are often used as a surrogate for fire intensity and are based on data and observations obtained from the field that represent short-term effects in the immediate environment after fire (Key and Benson, 2006; De Santis and Chuvieco, 2009; Estes *et al*., 2017). Fire severity may also be assessed using remotely sensed spectral indices combined with field measured metrics (Key and Benson, 2006; De Santis and Chuvieco, 2009; French *et al*., 2008). Studies of fire severity vary according to the type of ecosystem under assessment, but most often emphasise the overall loss of organic matter (biomass) both above- and belowground (Keeley, 2009).

Fire can also cause changes in carbon (C) and nutrient pools through heating (volatilisation) and combustion of biomass. Changes in C and nutrients due to biomass burning has flow-on effects for ecosystem cycling (Bird *et al*., 2015). The link between measures of fire severity and the impact on ecosystem processes involving C and nutrients are often complex and not easy to determine (Kitzberger *et al*., 2005; Huang and Boerner, 2007). Direct impacts of fire on pools of C and nutrients in forests are generally easier to quantify. Ash and char production can be used as a broad indicator of the temperature reached or heat produced during a fire and can be a key factor in understanding impacts on nutrient cycling and landscape recovery (Bento-Goncalves *et al*., 2012). Recent studies have investigated changes in ash characteristics, such as colour and fragment size, as an indicator of fire severity (Úbeda *et al*., 2009; Roy *et al*., 2010; Pereira *et al*., 2012; Dūdaité *et al*., 2013; Thomaz, 2018). Ash colour can reflect the severity of fire in the immediate area and can range from heterogenous black ash (char) produced from lower intensity fires through to fine, homogenous white-grey ash produced during higher intensity fires (Úbeda *et al*., 2009; Pereira *et al*., 2012; Bodí *et al*., 2014; Santin *et al*., 2015). The latter state is a good indicator that complete combustion has occurred. The problem encountered here is that determination of the colour of char and ash is subjective – colour can be perceived and described differently, even when matching against a standard set of colours. In addition, surrounding lighting can make a considerable difference to how the colour of a given material is observed.

Spectral analysis of soil has been used to determine a variety of soil attributes, such as inorganic soil constituents (e.g. hydroxides, methylenes, sulphur oxides, ammonium compounds), soil pH and electrical conductivity, cation exchange capacity, soil pedology (clay, sand and silt content), exchangeable aluminium and potassium, moisture content and organic carbon (Viscarra Rossel *et al.,* 2006; Stenberg *et al*., 2010). These studies highlight the potential use of infrared spectroscopy to determine inorganic and organic features of samples and its suitability for other environmental applications (Clark, 1999; Rossel, 2007; 2009; Vergnoux *et al*., 2009; Perez-Bejarano and

Guerrero, 2018; Liu *et al*., 2019). Visible and near infrared (NIR) reflectance regions can detect combinations and overtones of vibrational frequencies of bonds in molecules in materials. This includes bond vibrations between oxygen and hydrogen (OH), carbon and hydrogen (CH), and nitrogen and hydrogen (NH) which results in indicative NIR absorbance bands (Burns and Ciurczak, 2007). Using NIR to describe residues from combustion can provide useful information about the associated mineralogy of samples such as char and ash deposited post-fire (Brook and Wittenberg, 2016; Skvaril *et al*., 2017).

With the increased availability and reduced cost of handheld NIR scanners, there is potential for this technology to be used as a tool in the field to investigate both chemical and physical properties of ash. Spectroscopy data collected from char and ash from fire could, in theory, be used to estimate losses and changes in availability of C, nitrogen (N) and other nutrients from an ecosystem (Liu *et al*., 2019).

The aim of the study presented here is to determine whether spectroscopy data of fire by-products (char and ash) can be used as a fire severity metric. Colour matching of residues, a common method for rapid assessment of ash properties, is generally done subjectively using some form of universal colour comparison (e.g. Munsell colour system). The method presented here will eliminate human bias for colour matching. Spectroscopy data will also be used to investigate changes in the C content of residues. Background information and baseline data for this investigation have been presented in Milestone 2.3.4 (Final report on advances in soil carbon fingerprinting – Quantifying the conversion of vegetation to ash for soil carbon fingerprinting; Parnell *et al*., 2020a) and Milestone 3.1.4 (Draft report on soil carbon and fire severity – Ash colour as a fire severity metric; Parnell *et al*., 2020b), respectively.

2. METHODS

2.1 SAMPLE COLLECTION

Trial material

Bulked samples of three dominant types of surface fuels (leaves, twigs and bark) were collected from various locations. The three broad types of fuels were further separated according to physical features of each type of fuel. Leaves were classified as 'curly' (*Eucalyptus saligna*), 'flat' (a mixture of leaves from dry sclerophyll forest), and two types of 'needle-like' leaves (Pine needles and Casuarina phyllodes; Table 1). Twigs were separated into size classes: 0-2.5, 2.5-5.0 and >5.0 mm diameter (thin, medium and thick, respectively). Different types of bark were collected from several tree species based on varying thickness and density (Paperbark, Smooth bark – Red Gum, Smooth bark – Blue Gum and Rough bark – Turpentine; Table 1).

Table 1. Collection location, species and descriptions of surface fuel (trial and field) samples collected for the study. All collection sites were in New South Wales.

Category	Collection location	Species	Descriptive name
Leaves	Richmond	*Eucalyptus saligna*	Curly leaves
Leaves	Hornsby	Assorted – *Angophora costata, E. saligna, Syncarpia glomulifera*	Flat leaves
Leaves	Cobbitty	*Pinus radiata*	Pine needles
Leaves	Eveleigh	*Allocasuarina cunninghamiana*	Casuarina phyllodes
Twigs	Hornsby	Assorted – *A. costata, E. saligna, S. glomulifera*	0-2.5 mm (thin)
Twigs	Hornsby	Assorted – *A. costata, E. saligna, S. glomulifera*	2.5-5.0 mm (medium)
Twigs	Hornsby	Assorted – *A. costata, E. saligna, S. glomulifera*	>5.0 mm (thick)
Bark	Eveleigh	*Melaleuca quinquenervia*	Paperbark
Bark	Hornsby	*A. costata*	Smooth bark – Red Gum
Bark	Hornsby	*E. saligna*	Smooth bark – Blue Gum
Bark	Hornsby	*S. glomulifera*	Rough bark – Turpentine
Leaves	Blue Mountains	Assorted species	Leaves
Bark	Blue Mountains	Assorted species	Bark
Twigs	Blue Mountains	Assorted species	Twigs (2.5-5.0 mm)
Fine fuel	Blue Mountains	Assorted species	Fine fuel (<0.9 mm)
Soil	Blue Mountains	Assorted species	Soil (<0.2 mm)

Field material

Field samples were collected from three unburnt plots from a site located on the southern side of the Blue Mountains (34°19'12.0"S, 150°28'12.0"E; 613 m above sea level) (Rocky Waterholes, see Bell *et al*., 2020 for further details). The forest is broadly classified as a Dry Sclerophyll Forest and the predominant species are a variety of eucalypts, wattles and banksias. Surface fuel samples were collected using a circular sampling ring (0.1 m^2) and were bagged separately into leaves, twigs, bark, soil and fine fuel. Samples were oven-dried for 48 h at 60 °C and then passed through a 9 mm sieve to ensure that each grouping only consisted of that specific material. Soil samples were sieved using a 2 mm sieve to remove any roots and rocks.

2.3 SAMPLE PREPARATION AND HEATING

Samples were oven-dried at 70 °C for 3 days. Dried samples were kept in a desiccator when removed from the oven and prior to heating in the muffle furnace to prevent absorption of moisture from the atmosphere. Subsamples of each fuel type (approximately 2.0 g, n = 8) were weighed into foil trays and heated in a muffle furnace at 100, 200, 300, 400, 500 and 600 °C for 60 min. Samples were cooled until they could be handled safely and reweighed to determine weight loss then stored for later analysis. The control samples (referred to as 'unburnt') represented surface fuel or soil that was not heated or combusted and were held at 25 °C.

2.4 COLOUR ANALYSIS

Residues of surface fuels and soil remaining after heating and combustion were classified according to the Munsell colour system (Munsell Colour Company, 1950). This is a system that has been widely used in soil science for classification of diverse soil types. Past studies have also adopted this method to classify ash from biomass heated at different temperatures (Úbeda *et al*., 2009; Dūdaité *et al*., 2011; Balfour, 2013; Bodí *et al*., 2014). Under fluorescent light, ground material was compared to the Munsell soil colour chart to determine the associated hue value and chromas at each temperature. Photographs were also taken with and without flash for a secondary reference. Visually matched Munsell colour scores have been presented previously in Parnell *et al*. (2020a). These scores were imported into R (R Core Team, 2020) and converted into generated Munsell colours, using the "munsell" package (Whickham, 2018). Black, greys and whites that were in the grey range from the visual readings were converted in R into the range of N 1/0 to N 10/0 (black to white).

2.5 SPECTROSCOPY DATA

Small portions of ground samples were placed on clean aluminium foil and scanned using a portable spectroradiometer with a fitted handheld contact probe for spectral analysis (PSR+ 3500 Portable Spectroradiometer; Spectral Evolution, Massachusetts, United States). Spectral analysis was performed in the visible to shortwave infrared wavelength range (350-2500 nm) with measurements taken at 1 nm intervals. Each sample was scanned five times to reduce variance among scans. A white reference panel was scanned before each sample. Scans were analysed using the DARWin SP Application Software (V1.3, Spectral Evolution, Massachusetts, United States).

2.6 NEAR INFRARED COLOURING

Reflectance spectral data from between the range of 350 and 830 nm were averaged over interval ranges of 5 nm. The values were then divided by 100 to change reflectance (%) into proportions (CIE 1976; International Commission on Illumination, CIE, Vienna, Austria). Tristimulus values (X, Y, and Z) were determined from the averaged values using the standard illuminant E spectral power distribution (equal-energy radiator) as the visible light source (Smith and Guild, 1931). The X, Y, Z tristimulus values were then converted to the CIE 1976 L*a*b* uniform colour space where L* indicates lightness from black (0) to white (100), a* is the red (+)/green (-) coordinate and b* is the yellow (+)/blue (-) coordinate (McLaren, 1976).

L*a*b* colour values were used as input values in Adobe Photoshop CC (2015.1.2 release; Adobe Inc., San Jose, California, United States) to create a coloured square to visualise the colour observed from NIR scans.

2.7 PARTIAL LEAST SQUARES REGRESSION FOR ESTIMATION

A partial least squares (PLS) regression model was generated in R using the 'pls' (v. 2.7-2; Mevik, 2019) and plsVarSel (v. 0.9.5; Mehmood *et al.*, 2012) packages. Each PLS regression model was created using a generic algorithm that randomly selects wavelengths from the NIR spectroscopy scans and retains those that continually show high performance when correlated against either C or N content or temperature values (Mehmood *et al.*, 2012).

3. RESULTS AND DISCUSSION

3.1 MUNSELL COLOUR MATCHING

The Munsell colour system was developed to describe perception of colour by the human eye (Munsell Colour Company, 1950). Modern-day computerised colour matching systems have been widely adopted in science to improve uniformity of colour selection. The hue values and chromas identified for heated and combusted samples representing different fuel types and the corresponding colour match generated using R are presented in Figure 1.

Samples of different fuel types heated to temperatures of 100 and 200 °C showed only small difference in physical properties and colour compared to their unburnt counterparts, mainly only as a slight darkening when heated at 200 °C (Figure 1). When heated to 300 °C, most fuel types were completely charred and appeared dark brown to black in colour (i.e. N 1/0). This colour represents incomplete combustion (Khanna *et al*., 1994). At 400 °C, half of the fuel types (flat leaves, Casuarina cladodes, all twigs and smooth bark from Red Gum) had decomposed into a fine grey or white powdery ash (N 5/0 through to N 9/0) indicating almost complete combustion, a state where most of the organic compounds had been removed (Úbeda *et al*., 2009; Pereira *et al*., 2012; Bodí *et al*., 2014; Santin *et al*., 2015). These types of fuel showed minimal or no additional change in colour when heated at temperatures above 400 °C. Of the five fuel types which had not been fully combusted at 400 °C, three of them (Pine needles, smooth bark from Blue Gum and rough bark from Turpentine) were a fine white (N 10/0) or grey ash (N 8/0 or N 9/0) when heated at 600 °C. At this temperature, residues from two fuel types (curly leaves and Paperbark) were fine and powdery in texture, as for other fuel types, but remained light brown in colour (Figure 1).

Surface fuels (leaves, bark, fine fuel and twigs) and soil collected from the field showed similar changes in physical properties and colour gradation of residues when compared to the trial material (Figure 2). There were minimal differences in colour change when heated at lower temperatures of 100 and 200 °C, with darkening of material and charring occurring at 300 °C. Soil was the only material which did not show signs of charring at 300 °C but it did darken from its initial state (10YR 4/2). Between 400 and 500 °C, soil colour was lighter than the control (heated at 25 °C) and, at 600 °C, was darker and more orange as the hue changed from 10YR to 7.5YR (Figure 2). This process of darkening and lightening is consistent with the literature as rubification occurs at higher temperatures where the transformation of iron compounds in soils to free iron oxides start to occur (Liedgren, 2017). In general, surface fuels collected from the field had fine ash residues that were pale or light brown in colour when combusted at 500 and 600 °C (Figure 2) but were not white or grey ash as expected.

Differences in colours of residues, particularly when fuels were combusted at higher temperatures, may be due to species composition. Fuel samples collected from the field were separated according to physical features (leaves, twigs, bark and fine fuel) and may have represented a range of species. As a result, this could affect not only the colour of ash, but also the chemical properties of residues remaining at higher temperatures. For example, in other studies, differences were found between

chemical properties of ash produced from combustion of needles of *Pinus sylvestris* and leaf litter from *Acer platanoides* (Dūdaitė *et al*., 2013). Khanna *et al*. (1994) found ash produced by burning litter from a *Eucalyptus* forest to be highly variable as did Mastrolonardo *et al*. (2017) for ash from mixed forest (dominated by Downy Oak (*Quercus pubescentis*) and Maritime Pine (*Pinus pinaster*)) in Italy.

Besides the notion of species effect, another assumption worth discussing involves the 'state' of the material used. Some of the surface fuel samples collected as trial material represented a single species (e.g. all curly leaves were from *Eucalyptus saligna*, pine needles were collected from *Pinus radiata*, different types of bark were collected from separate species), were generally newly fallen and were gathered at a single point in time. Although field material was collected within a two-day period, it was much more heterogeneous in nature according to species composition and age and state of decomposition as it may have been newly fallen or on the ground for longer periods of time. There are at least two stages of decomposition of plant litter. The early stage of decomposition involves leaching of soluble compounds and decomposition of soluble and non-lignified cellulose and hemicellulose, and the later stage is when degradation of lignified tissue occurs (Couteaux *et al*., 1995; Heim and Frey, 2004). Composition and age of fuel samples can influence the way the sample is burnt and the resulting chemical composition of ash (Mao *et al*., 2017).

It should also be noted here that it is well recognised that combustion of plant biomass in a muffle furnace is not the same as what might happen in the field (Qian *et al*., 2009; Bodí *et al*., 2011; Hogue and Inglett, 2012). Residues are more homogenous when heat can be applied for a greater period of time and chemical reactions that occur during combustion are more complete. With flaming combustion, fuels are subject to different amounts of heat for different periods of time and will result in much more heterogenous residues. To overcome this, some laboratory studies try to mimic burning in the field by combusting material in an open vessel (e.g. Gabet and Bookter, 2011).

Figure 1. Description of colour as hue value and chroma for each of the representative trial fuel types when heated or combusted at six different temperatures using the Munsell soil colour chart (Munsell Colour Company, 1950). The Munsell colour notation is as follows: R = Red, YR = Yellow-Red, Y = Yellow, B = Blue, PB = Purple-Blue and N = neutral.

Figure 2. Description of colour as hue value and chroma for each of the fuel types collected from the field when heated or combusted at six different temperatures using the Munsell soil colour chart (Munsell Colour Company, 1950). The Munsell colour notation is as follows: R = Red, YR = Yellow-Red, Y = Yellow, B = Blue, PB = Purple-Blue and N = neutral.

3.2 NEAR INFRARED SPECTROSCOPY

Reflectance patterns

Using near infrared spectroscopy, there is potential to distinguish both similarities and differences in residues produced from heating and combustion. At wavelengths ranging from 350 to 2500 nm, peaks and declines in reflectance can be matched with the presence of certain chemicals in materials (Viscarra Rossel *et al*., 2006; Teye *et al*., 2013; Jamshidi, 2017). Spectroscopic scans of residues produced after heating and combustion of trial fuels are provided in Figure 3.

There are striking similarities in patterns of peaks for all fuels when unburnt (Figure 3b) and after heating or combustion at 100, 200 and 300 °C (Figure 3c, d, e). An exception to this was found for Paperbark heated at 100 °C. The spike in reflectance between 2000 and 2500 nm for this fuel type was comparable to residues from leaves and other bark heated at 400 °C (Figure 3f). Based on similarities in spectroscopic data, it could be inferred that chemical changes occurring in Paperbark at low temperatures are similar to changes occurring in other fuels at a higher temperature. This could be anything from volatilisation of soluble nutrients (i.e. N) to thermal decomposition of various plant cell components (i.e. cellulose, hemicellulose and lignin).

At the highest temperatures, 500 and 600 °C, although each fuel type had varying reflectance peaks at different wavelengths, their respective groupings (leaves, twigs, bark) were relatively consistent at a given wavelength (Figure 3g, h). The exception was for ash from smooth bark from Red Gum when combusted at 500 °C, where there were no significant peaks detected at any wavelength and the lowest reflectance values were recorded (25-35%) (Figure 3g).

Surface fuel samples collected from the field varied considerably when compared to the trial material (Figure 4). Overall, the reflectance values were smaller, with the highest peak being 180% at 500 °C for wavelengths between 2000 and 2500 nm (Figure 4f). In contrast, the highest peak in trial material occurred at 400 °C in the same wavelength range (600%; Figure 3f). Fine fuel and soil had the lowest reflectance of all surface fuel types and had similar peaks for the 350-2500 nm wavelength range when unburnt or heated to 100 °C (Figure 4a, b). Under the same conditions, leaves, twigs and bark had similar patterns of peaks with higher reflectance than soil and fine fuel, but all fuel types had similar reflectance at 200 °C (Figure 4c). Residues formed from combustion of both soil and surface fuel at 500 and 600 °C had a similar range of reflectance values and patterns (Figure 4d, e, f, g).

The reflectance patterns of residues from the trial material combusted at 500 and 600 °C were markedly different from their respective counterparts collected from the field (Figure 3 and 4). As discussed previously, this could be due, in part, to the different stages of decomposition of the plant materials collected (Couteaux *et al*., 1995; Heim and Frey, 2004; Mao *et al*., 2017).

Colour matching

Reflectance values between 350 and 830 nm were analysed using a spectral calculator to determine the respective L*a*b* colour coordinates. L*a*b* coordinates determine the lightness (L), red/green (A) and the yellow/blue (B) spectrum of the sample. The resulting L*a*b* colour values from the NIR scans from the trial material (Figure 5) and the field material (Figure 6) are presented.

For the trial material, only a small colour change occurred when heated at 100 and 200 °C, with all the samples darkening at the higher temperature (Figure 5). When combusted at 300 °C, all samples were black, ranging from jet black to clouded black, and at 400 °C, and for all samples the L*a*b* colour had lightened with residues from flat leaves and Paperbark remaining dark grey (Figure 5). At 500 and 600 °C, surface fuels had reached their final stage of combustion and the lightest L*a*b* colours were observed. The exceptions were curly leaves, Pine needles, smooth bark from Blue Gum and thin twigs, where the L*a*b* shade at 600 °C was darker than the colour developed at 500 °C (Figure 5).

Despite heating and combusting replicate surface fuel samples under controlled conditions in a muffle furnace there was variation among residues, both in particle size and colour, within a given fuel type (see Figure 7 for examples of heterogenous residues). Some of the replicate samples showed varying degrees of charring (indicated by black particles of varying size) when combusted at temperatures between 400 and 600 °C while others were completely converted to fine homogenous ash. As each L*a*b* colour coordinate is an average of five replicate NIR scans from each sample, it is possible that this physical and colour variation was captured and reflected in slightly different shades. This raises the question of the sensitivity of NIR scanning and the possible need for 'step changes' in colour rather than 'gradational changes' to indicate the degree of thermal decomposition of fuel.

Surface fuels collected from the field showed a similar pattern to the trial material with the residues from heating at 100 and 200 °C darkening only slightly in their L*a*b* coordinates. At 300 °C, a deep brown/black colour was observed for leaves, fine fuel, bark and twigs (Figure 6) rather than the expected range of black observed for the trial surface fuels. With combustion at 400 to 600 °C, the residue colour increased in lightness resulting in a range from grey brown to a light brown with red yellow undertones (Figure 6). In contrast, residues of combusted soil were orange brown in colour due to the process of iron oxidation, as discussed previously.

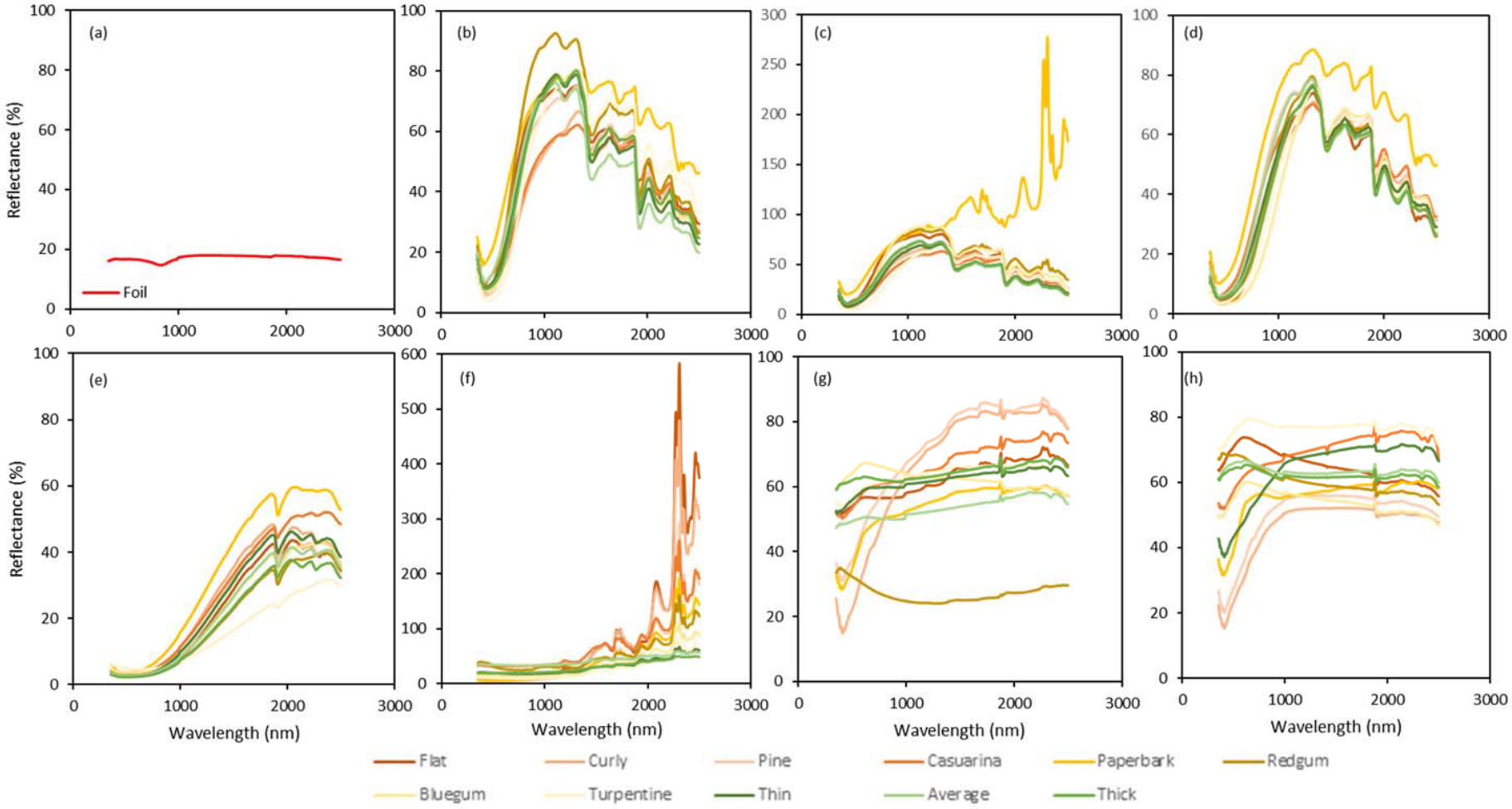

Figure 3. Reflectance values from trial material of surface fuels for (a) foil background standard, (b) unburnt material, (c) samples burnt at 100 °C, (d) 200 °C, (e) 300 °C, (f) 400 °C, (g) 500 °C, and (h) 600 °C, between 350 and 2500 nm. Values are indicative of an average of five replicate scans. Note variation in maximum reflectance values.

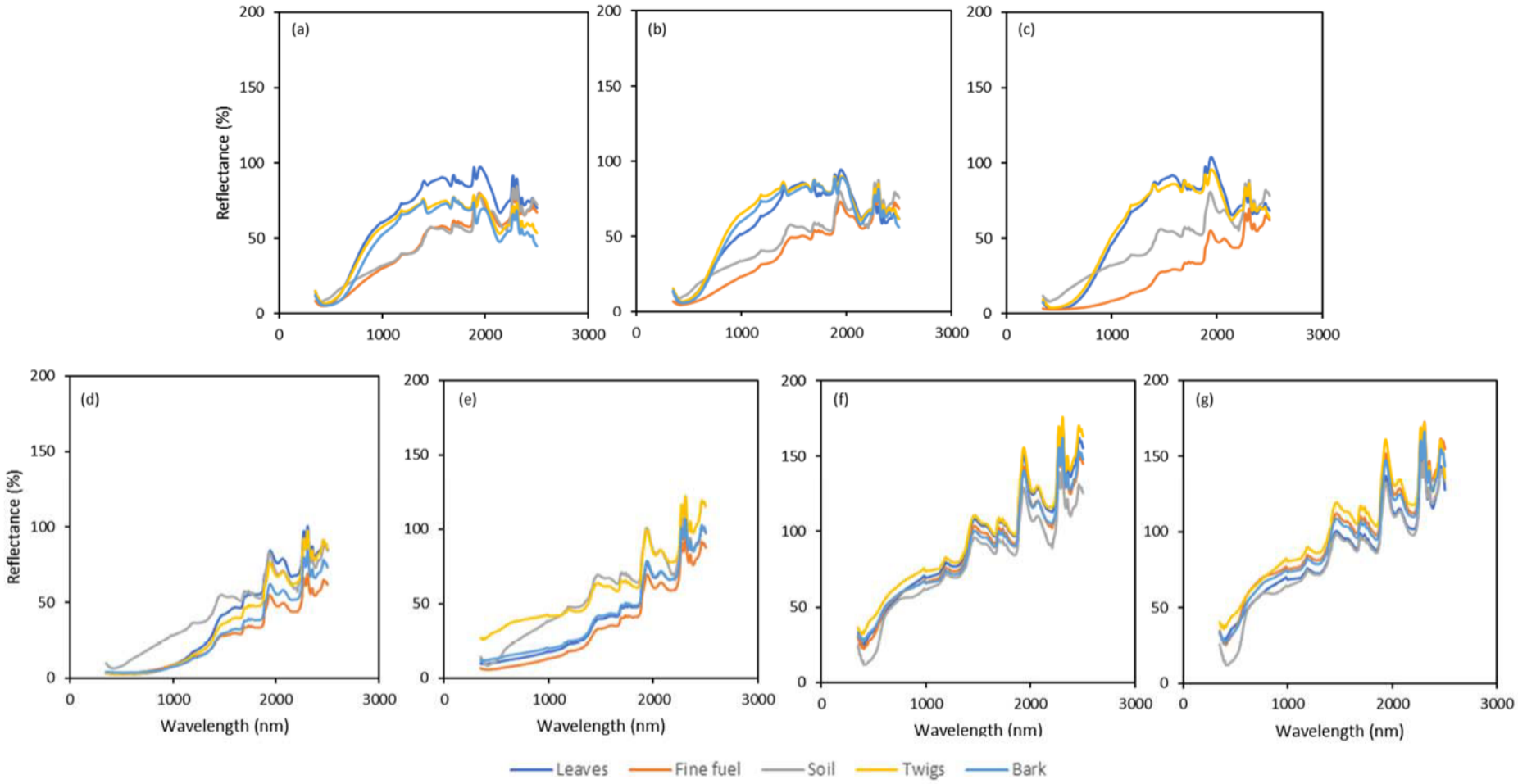

Figure 4. Reflectance values of surface fuels collected from the field for (a) unburnt material, (b) samples burnt at 100 °C, (c) 200 °C, (d) 300 °C, (e) 400 °C, (f) 500 °C, and (g) 600 °C, between 350 and 2500 nm. Values are an average of five replicate scans.

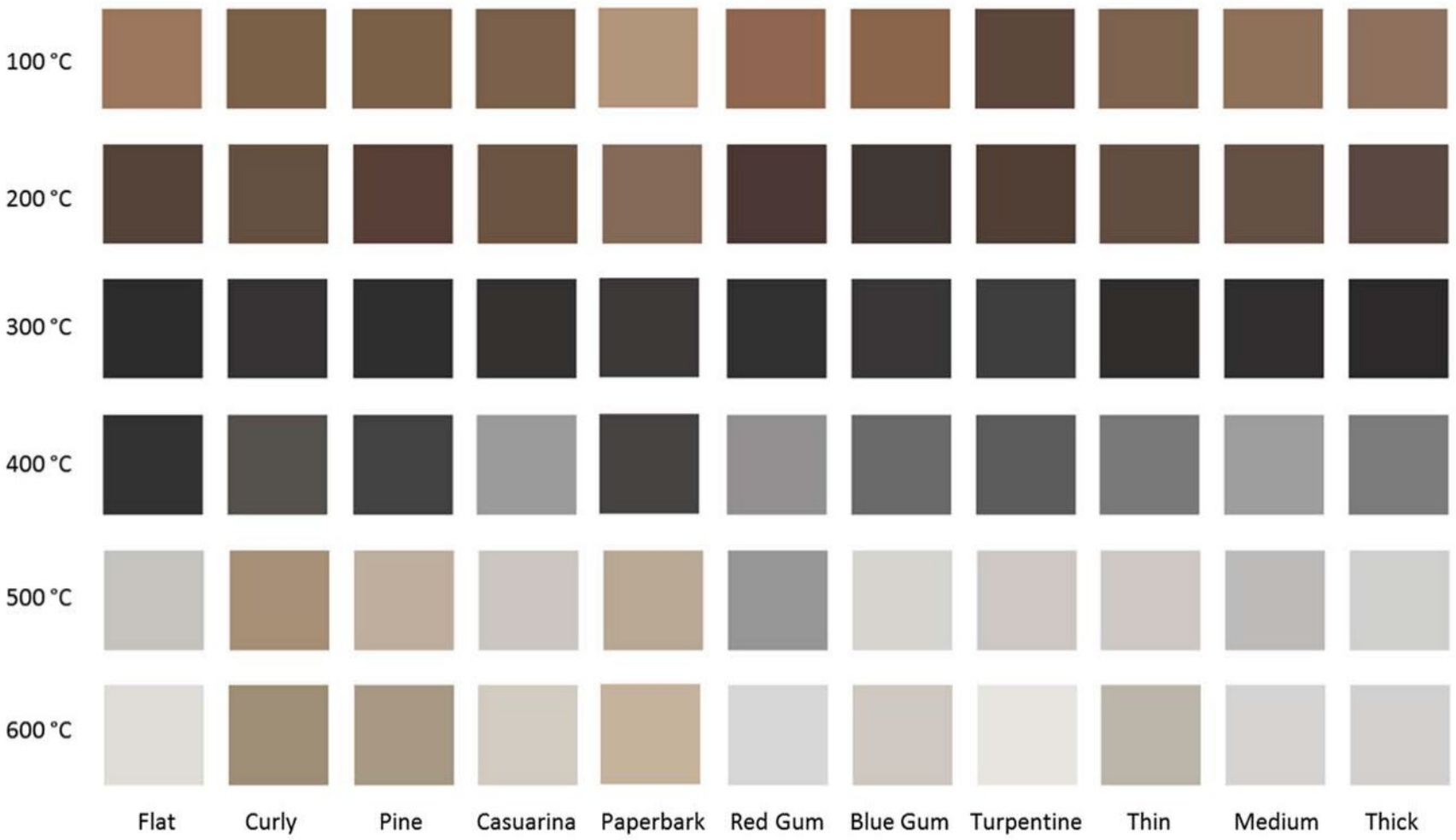

Figure 5. L*a*b* colours derived from data extracted from near infrared spectroscopy of residues from different types of surface fuels used as trial materials (leaves, twigs and bark) when heated and combusted at temperatures between 100 and 600 °C.

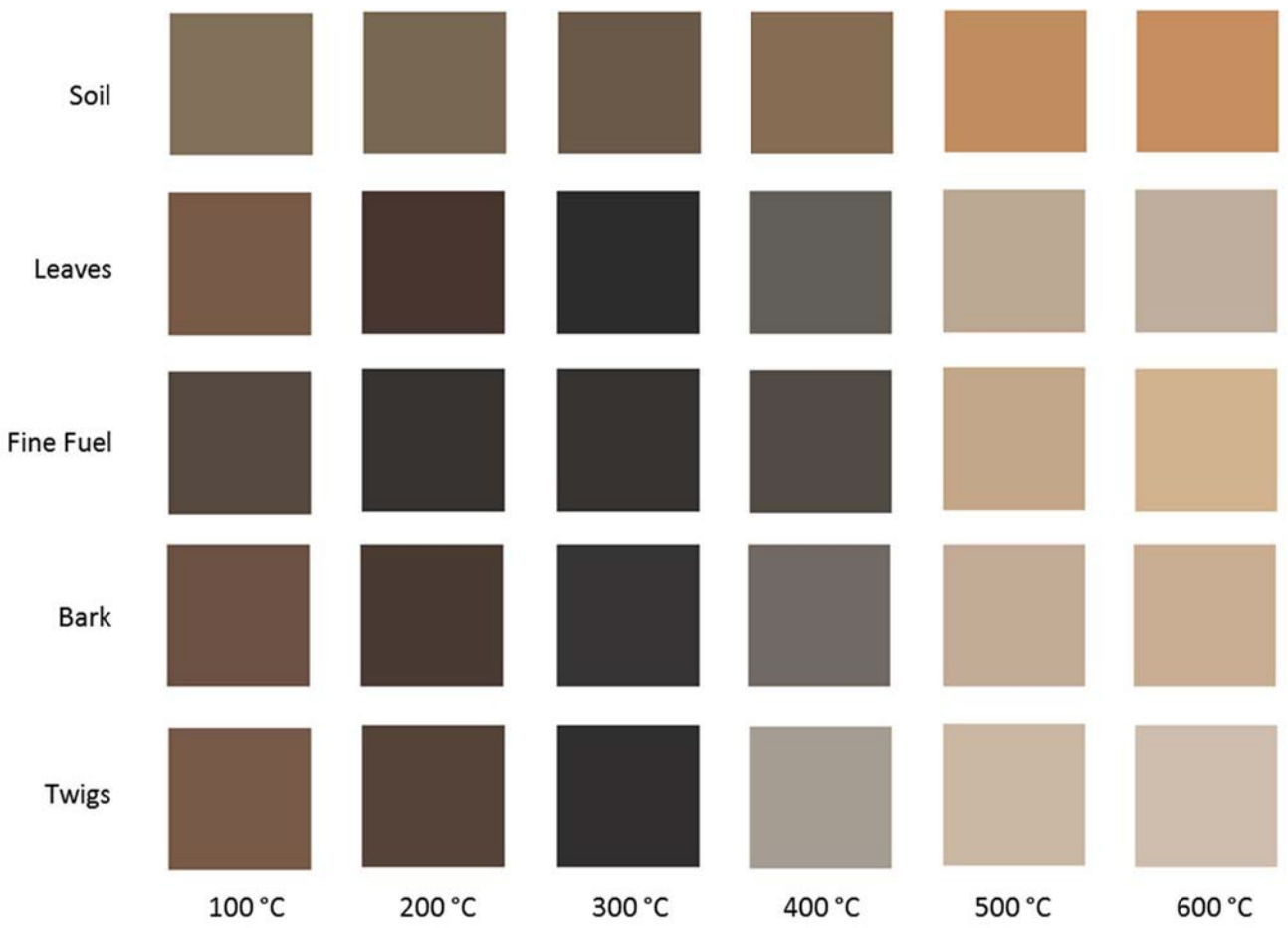

Figure 6. L*a*b* colours derived from data extracted from near infrared spectroscopy of residues from different types of surface fuels collected from the field (soil, leaves, fine fuel, bark and twigs) when heated and combusted at temperatures between 100 and 600 °C.

3.3 COMPARISON OF MUNSELL AND NEAR INFRARED COLOURS

Using the 'munsell' R package (Wickham, 2018), it was evident that there are discrepancies in manually converting visual colours into computer-generated colours. The ability to convert grey colours from visual scores to R was limited as the various undertones of grey, yellow and red viewed in person could not be translated successfully. For example, a grey which had a blue undertone was translated the same way as a grey which had a yellow/red undertone (Figure 7). The way that the package selects colours also slightly differs to the Munsell soil colour chart used, as the package only allows chroma to increase by increments of 2 while the manual colour chart allowed the capacity to increase one increment at a time. This caused misalignment, albeit slight, between the actual colour of the sample and Munsell colour value. An example of this can be seen in Figure 7b. The residue colour of rough bark from Turpentine was calculated to be olive green using the R conversion of Munsell colour compared to the L*a*b* counterpart derived from NIR spectroscopy which was much closer to the actual colour.

Many previous studies have attempted to determine how well individuals (experienced and novice) are able to manually match Munsell colour charts with soil. It has been suggested that only experienced soil scientists can interpolate between Munsell colour charts to the nearest hue and half unit of value and chroma (Pomerening and Knox, 1962; Shields *et al*., 1966; Cooper, 1990; Post *et al.*, 1993; 2006; Rabenhorst *et al.*, 2014). It has been identified that soil colour observed using Munsell soil colour charts are strongly influenced by the environmental conditions in which they are measured (illumination) and by the experience and colour vision of the observer (i.e. normal and colour blind), creating a subjective measurement which can create inconsistencies between individuals (Stiglitz *et al*., 2016).

Although Munsell colour matching has been used in soil science for decades, advancements in modern technology have permitted greater precision in the measurement of colours, eliminating the need for subjective visual assessment and removing the limitation in the range of colour tones available. As an alternative, the CIE L*a*b* system has been developed and trialled (Kirillova *et al.*, 2015). The system is physically-based, mathematically-oriented and can be more reliable than colour charts due to the closeness it has to human vision (Marques-Mateu *et al*., 2018). From the study presented here, we support the use of the L*a*b* colour system to characterise char and ash residues from combustion of surface fuels and encourage further testing to use portable NIR scanning to determine fire severity in the field.

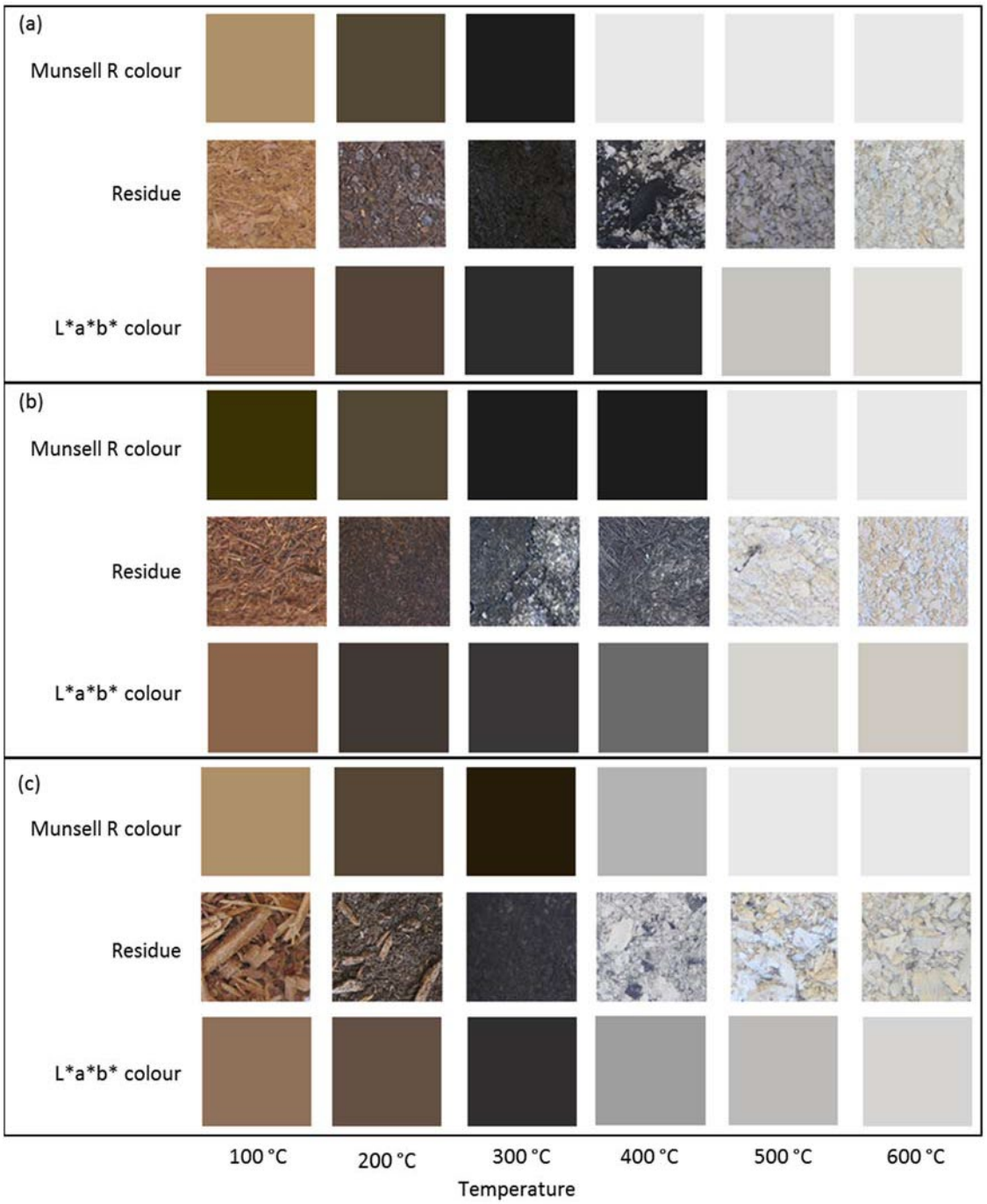

Figure 7. Comparisons of Munsell colours, residues and L*a*b* colour of (a) flat leaves, (b) rough bark from Turpentine, and (c) medium twigs, from the trial material burnt at temperatures between 100 and 600 °C.

3.4 USING NEAR INFRARED TO PREDICT CARBON, NITROGEN AND TEMPERATURE OF RESIDUE FORMATION

To develop predictions of C and N content of residues and the temperature that it was formed at from the NIR scans, a partial least squares (PLS) regression model was used. Partial least squares regressions are used to build models which make predictions from more than one dependent variable (Long, 2013). Regression models using PLS have x and y values selected to maximise the correlation between scores of x and y variables. In this instance, the PLS was generated to build an equation that can predict laboratory data (C, N and temperature) based on spectral data (wavelengths).

The data was analysed together as a large grouping in the PLS regression model instead of being analysed individually in their logical groupings (e.g. fuel type, heating or combustion temperature and respective %C and %N values). This approach was taken to emulate a 'real world' prediction as contributing components are likely to be mixed and, as such, a prediction that incorporates a combined analysis of all materials would hypothetically provide a more accurate prediction. In contrast, separate PLS regression models were developed for surface fuels from both the trial and field collected materials. Resulting model metrics are shown in Table 2.

Table 2. Model metrics of a partial least squares (PLS) regression model of predicted values and carbon, nitrogen and temperature data derived from trial material and surface fuels collected from the field. Components = number of components selected in the PLS regression, RMSE = residual mean squared error, R^2 = r-squared value, MAE = mean absolute error

Variable	Components	RMSE	R^2	MAE
Trial surface fuels				
Carbon (%)	7	9.66	0.79	7.34
Nitrogen (%)	6	0.45	0.53	0.30
Temperature (°C)	6	66.70	0.88	50.05
Field collected surface fuels				
Carbon (%)	2	10.33	0.69	8.36
Nitrogen (%)	7	0.16	0.69	0.09
Temperature (°C)	7	62.73	0.90	50.18

Partial least squares regression models related to temperatures at which residues were produced resulted in better predictions for both trial and field material with R^2 values of 0.88 and 0.90, respectively. The PSL regression modelling had a mean absolute error (MAE) of 50 °C for both field and trial material, and errors of 63 and 67 °C for the predicted values (Table 2). This means that if a temperature of 350 °C was predicted according to the NIR scan of a given residue, the actual temperature may have been between 300 and 400 °C.

The PLS regression model for C content (%C) in surface fuels collected from the field had a lower R^2 value (0.69) coupled with a higher error (8.4 %C) compared to the model for the trial material (R^2 = 0.79, error = 7.3 %C) (Table 2). As measured values of %C in residues from the trial fuel samples varied from 48-58 %C in unburnt fuels and those heated at 100 and 200 °C (Parnell *et al*., 2020a), this error represents predictions of %C being within a range of 41-65 %C. When trial surface fuels were combusted at 300 °C and analysed, they contained from 50-75 %C depending on fuel type. For example, Paperbark, medium and thick twigs all had 50 %C or lower (Parnell *et al*., 2020a). This means predictive values based on NIR scans could range from 43-82 %C. At higher temperatures, small amounts of

C, generally less than 10%, remained in ash residues suggesting that the predicted amounts of C could be far less (2 %C) to nearly double (18 %C) what might be reasonably expected. In this case, the predicted error is relatively more important for ash residues with low C content.

A similar situation applies for prediction of N content in residues. Prior to heating of most surface fuels, measured N content was low (0.5-1.2 %N) (Parnell *et al*., 2020a) which, when coupled with a MAE of 0.09 %N for trial surface fuel samples, represents a predictive range from NIR scans of 0.4-1.3 %N. For surface fuels collected from the field, the associated MAE was higher (0.30%; Table 2) suggesting that the predictive range of N% is less accurate and ranges from 0.2-1.5 %N. The MAE is much more important when considering residues with low amounts of C and N.

Using the PLS regression models developed, predictions and respective measured values of %C, %N and temperature (°C) data were correlated (Figure 8). As examples of how these predictive plots can be used, when trial samples are heated to a temperature of 180 °C, it is expected that there would be 44 %C and 0.4 %N remaining in heated materials; at 280 °C there would be 57 %C and 1 %N in charred residues, and at 633 °C there would be 1.1 %C and 0.07 %N in ash.

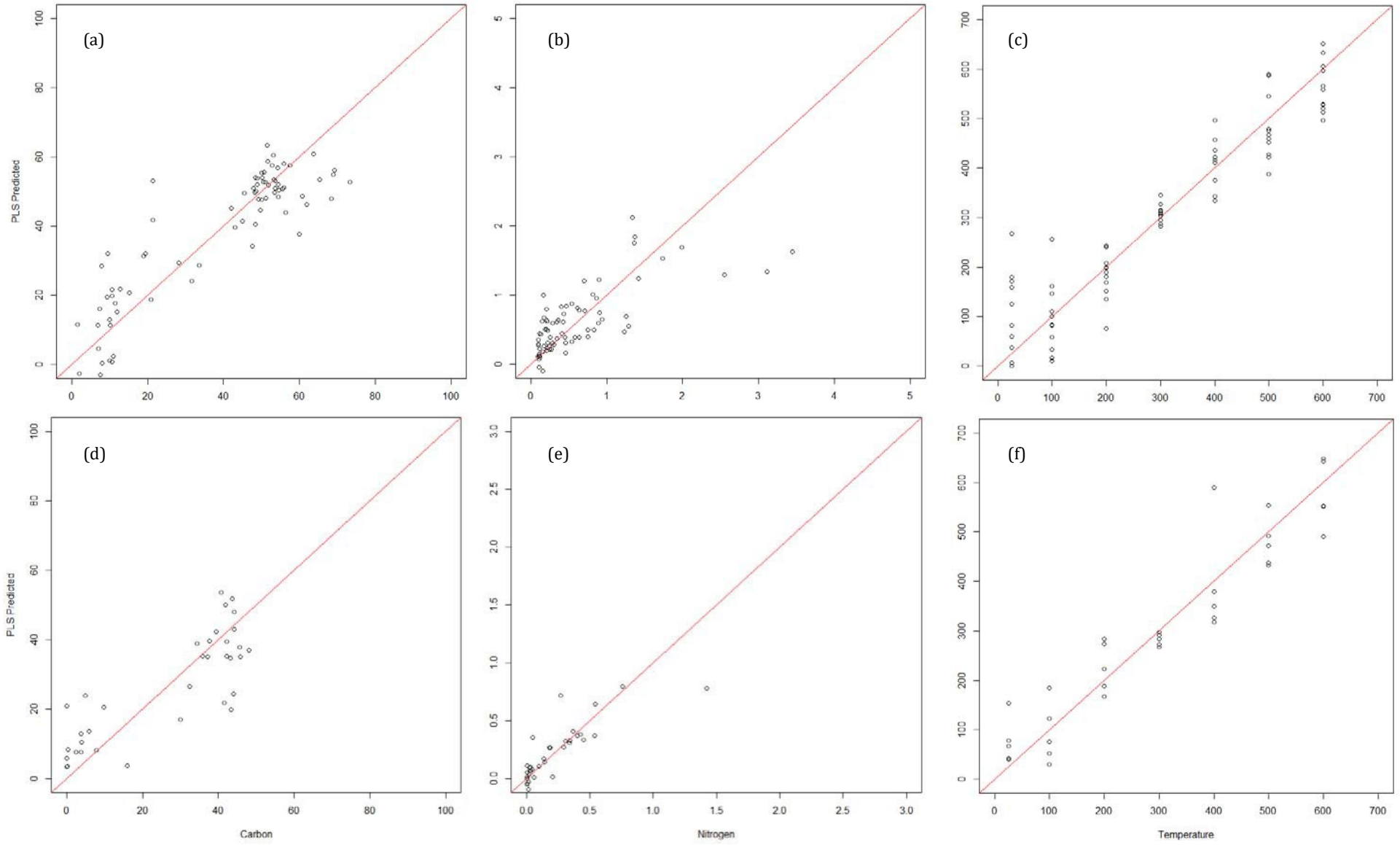

Figure 8. Linear regression plots displaying the correlation between measured carbon (%; a, d), nitrogen (%; b, e) and temperature (°C; c, f) data and predicted values for trial material (a, b, c) and field material (d, e, f). Predicted values were generated using partial least squares regression models developed using information from all fuel types and near infrared scans generated at all wavelengths[3].

4. CONCLUSIONS

The use of the Munsell colour system, though highly subjective, can provide useful indirect information about fire severity as there are distinct patterns among temperature and the colour of ash residues for Australian fuels. In this study, we have demonstrated that spectroscopy data from NIR scanners can be used to remove subjectivity associated with colour matching. As seen in the spectroscopic data, it is evident that there are identifiable peaks at different wavelengths, which could also provide insight into various chemical properties of residues and the implications that fires of different severity may have on ecosystem recovery. As demonstrated using PLS regression models, it is feasible to predict carbon and nitrogen in ash residues and the temperature at which fuels were combusted with NIR spectroscopy. This research can be used to justify further investigation of the use of handheld NIR systems in the field for determining fire severity.

ACKNOWLEDGMENTS

The authors would like to thank Honour student, Michelle Wang from the University of Sydney for her contribution to the research presented in this report. They would also like to acknowledge the following people from the University of Sydney: Michael Turner for his advice and technical assistance using the analytical equipment and muffle furnace; Mario Fajardo Pedraza and Liana Pozza for their help with Spectracus (extracting colours from NIR data); Jeremy Aditya Prananto, Ian Marang and Prof. Budiman Minasny for their help with the NIR spectrometer.

REFERENCES

1 Adey WH, Loveland K (2007) Community structure: biodiversity in model ecosystems. *Dynamic Aquaria Building and Restoring Living Ecosystems* 3, 173-189.

2 Bell T, Parnell D, Possell M (2020) Sampling and data analysis of field sites of 40 prescribed burns. Milestone 2.4.2 Technical Report, Bushfire and Natural Hazards Cooperative Research Centre, 23 p.

3 Bento-Goncalves A, Vieira A, Úbeda X, Martin D (2012) Fire and soils: key concepts and recent advances. *Geoderma* 191, 3-13.

4 Bird MI, Wynn JG, Saiz G, Wurster CM, McBeath A (2015) The pyrogenic carbon cycle. *Annual Review of Earth and Planetary Sciences* 43, 273-298.

5 Bodí MB, Martin DA, Balfour VN, Santin C, Doerr SH, Pereira P, Cerda A, Mataix-Solera J (2014) Wildland fire ash: production, composition and eco-hydro-geomorphic effects. *Earth Science Review* 130, 103-127.

6 Bodí MB, Mataix-Solera J, Doerr SH, Cerdà A (2011) The wettability of ash from burned vegetation and its relationship to Mediterranean plant species type, burn severity and total organic carbon content. *Geoderma* 160, 599-607.

7 Brook A, Wittenberg L (2016) Ash-soil interface: mineralogical composition and physical structure. *Science of the Total Environment* 572, 1403-1413.

8 Burns DA, Ciurczak EW (2007) Handbook of Near-Infrared Analysis, Third Edition. *Practical Spectroscopy*, 340-370.

9 Clark RN (1999) Spectroscopy of rocks and minerals, and principles of spectroscopy. *Manual of Remote Sensing* 3, 3-58.

10 Couteaux MM, Bottner P, Berg B (1995) Litter decomposition, climate and litter quality. *Trends in Ecology and Evolution* 10, 63-66.

11 Cooper TH (1990) Development of students' abilities to match soil color to Munsell color chips. *Journal of Agronomic Education* 19, 141-144.

12 De Santis A, Chuvieco EG (2009) A modified version of the composite burn index for the initial assessment of the short-term burn severity from remotely sensed data. *Remote Sensing Environment* 113, 554-562.

13 Dūdaité J, Baltrenaite E, Úbeda X, Tamkeviciute M (2013) Effects of temperature on the properties of pine and maple leaf litter ash: a laboratory study. *Environmental Engineering and Management Journal* 12, 2107-2116.

14 Estes BL, Knapp EE, Skinner CN, Miller JD, Preissler HK (2017) Factors influencing fire severity under moderate burning conditions in the Klamath Mountains, Northern California, USA. *Ecosphere*, 8.

15 French NHF, Kasischke ES, Hall RJ, Murphy KA, Verbyla DL, Hoy EE, Allen JL (2008) Using landsat data to assess fire and burn severity in the north American boreal forest region: An overview and summary of results. *International Journal of Wildland Fire* 17, 443-462.

16 Gabet EJ, Bookter A (2011) Physical, chemical and hydrological properties of *Pinus ponderosa* ash. *International Journal of Wildland Fire* 20, 443-452.

17 Heim A, Frey B (2004) Early stage litter decomposition rates for Swiss forests. *Biogeochemistry* 70, 299-313.

18 Hogue BA, Inglett PW (2012) Nutrient release from combustion residues of two contrasting herbaceous vegetation types. *Science of the Total Environment* 431, 9-19.

19 Huang J, Boerner RE (2007) Effects of fire alone or combined with thinning on tissue nutrient concentrations and nutrient resorption in *Desmodium nudiflorum*. *Oecologia* 153, 233-243.

20 Jamshidi B (2017) Non-destructive safety assessment of agricultural products using Vis/NIR spectroscopy. *NIR News* 28, 4-8.

21 Khanna PK, Raison RJ, Falkiner RA (1994) Chemical properties of ash derived from *Eucalyptus* litter and its effects on forest soils. *Forest Ecology and Management* 66, 107-125.

22 Keeley JE (2008) Fire. Encyclopedia of Ecology, 1557-1564.

23 Keeley JE (2009) Fire intensity, fire severity and burn severity: a brief review and suggested use. *International Journal of Wildland Fire* 18, 116-126.

24 Key CH, Benson NC (2006) Landscape Assessment Firemon: Fire Effects Monitoring and Inventory System. U.S. Department of Agriculture, Forest Service, Rocky Mountain Research Station: Fort Collins, CO, USA.

25 Kirillova NP, Vodyanitskii YN, Sileva M (2015) Conversion of soil colour parameters from the Munsell system to the CIE-L*a*b system. *Eurasian Soil Science* 48, 468-475.

26 Kitzberger T, Raffaele E, Heinemann K, Mazzarino MJ (2005) Effects of fire severity in a north Patagonian subalpine forest. *Journal of Vegetation Science* 16, 5-12.

27 Liedgren L, Hornberg G, Magnusson T, Ostlund L (2017) Heat impact and soil colours beneath hearths in northern Sweden. *Journal of Archaeological Science* 79, 62-72.

28 Liu S, Shen H, Chen S, Zhao X, Biswas A, Jia X, Shi Z, Fang J (2019) Estimating forest soil organic carbon content using vis-NIR spectroscopy: implications for large-scale soil carbon spectroscopic assessment. *Geoderma* 348, 37-44.

29 Long FH (2013) Chapter 19: Multivariate analysis for metabolomics and proteomics data. In: *Proteomic and Metabolomic Approaches to Biomarker Discovery*, Issaq HJ, Veenstra TD (eds.) Academic Press, 299-311.

30 Mao B, Mao R, Zeng D-H (2017) Species diversity and chemical properties of litter influence non-additive effects of litter mixtures on soil carbon and nitrogen cycling. *PLoS ONE* 12, 1-19.

31 Marques-Mateu A, Moreno-Ramon H, Balasch S, Ibanez-Asensio S (2018) Quantifying the uncertainty of soil colour measurements with Munsell charts using a modified attribute agreement analysis. *Catena* 171, 44-53.

32 Mastrolonardo G, Hudspith VA, Francioso O, Rumpel C, Montecchio D, Doerr SH, Certini G (2017) Size fractionation as a tool for separating charcoal of different fuel source and recalcitrance in the wildfire ash layer. *Science of the Total Environment* 595, 461-471.

33 McLaren K (1976) XIII – The development of the CIE 1976 (L*a*b) uniform colour space and the colour-difference formula. *Journal of the Society of Dyers and Colourists* 92, 338-341.

34 Mehmood T, Liland KH, Snipen L, Sæbø S (2012) A review of variable selection: methods in partial least squares regression. *Chemometrics and Intelligent Laboratory Systems* 118, 62-69.

35 Mevik BH (2019) Introduction to the pls package. R package version 2.7.2. https://CRAN.R-project.org/package=pls

36 Munsell Colour Company (1950) Munsell soil colour charts. Macbeth Division of Kollmorgen Corporation, Baltimore, MD (revised 1975).

37 Parnell D, Bell T, Possell M (2020a) Quantifying the conversion of vegetation to ash for soil carbon fingerprinting. Milestone 2.3.4 Technical Report, Bushfire and Natural Hazards Cooperative Research Centre, 21 p.

38 Parnell D, Bell T, Possell M (2020b) Ash colour as a fire severity metric. Milestone 3.1.4 Draft

Report, Bushfire and Natural Hazards Cooperative Research Centre, 12 p.

39 Pereia P, Úbeda X, Martin DA (2012) Fire severity effects on ash chemical composition and water-extractable elements. *Geoderma* 191, 105-114.

40 Perez-Bejarano A, Guerrero C (2018) Near infrared spectroscopy to quantify the temperature reached in burned soils: importance of calibration set variability. *Geoderma* 326, 133-143.

41 Pointer MR (1981) A comparison of the CIE 1976 colour spaces. *Color Research and Application* 6, 2.

42 Pomerening JA, Knox EG (1962) Interpolation of Munsell soil color measurements. *Soil Science Society of America Proceedings* 26, 301-302.

43 Post DF, Bryant RB, Batchily AK, Levine SJ, Mays MD, Escadafal R (1993) Correlations between field and laboratory measurements of soil color. In: *Soil Color*, Bigham JM, Ciolkosz EJ (eds), SSSA Special Publication 31. SSSA, Madison, WI., 35-49.

44 Post DF, Parikh SJ, Papp RA, Ferriera L (2006) Evaluating the skill of students to determine soil morphology characteristics. *The Journal of Natural Resources and Life Sciences Education* 35, 217-224.

45 Qian Y, Miao SL, Gu B, Li YC (2009) Effects of burn temperature on ash nutrient forms and availability from Cattail (*Typha domingensis*) and Sawgrass (*Cladium jamaicense*) in the Florida Everglades. *Journal of Environmental Quality* 38, 451-464.

46 R Core Team (2020) R: A language and environment for statistical computing. R Foundation for Statistical Computing, Vienna, Austria. URL https://www.R-project.org/.

47 Rabenhorst MC, Matovich MM, Rossi AM, Fenstermacher DE (2014) Visual assessment and interpolation of low chroma soil colors. *Soil Science Society of America Journal* 78, 567-570.

48 Roy DP, Boschetti L, Maier SW, Smith AMS (2010) Field estimation of ash and char colour-lightness using a standard grey scale. *International Journal of Wildland Fire* 19, 698-704.

49 Rossel RV (2007) Robust modelling of soil diffuses reflectance spectra by "bagging-partial least squares regression". *Journal of Near Infrared Spectroscopy* 15, 39-47.

50 Rossel RV (2009) *In situ* measurements of soil colour, mineral composition and clay content by vis-NIR spectroscopy. *Geoderma* 150, 253-266.

51 Santin C, Doerr SH, Otero XL, Chafer CJ (2015) Quantity, composition and water contamination of potential ash produced under different wildfire severities. *Environmental Research* 142, 297-308.

52 Skvaril J, Kyprianidis K, Avelin A, Odlare M, Dahlquist E (2017) Fast determination of fuel properties in solid biofuel mixtures by near infrared spectroscopy. *Energy Procedia* 105, 1309-1317.

53 Shields JA, St. Arnaud RJ, Paul EA, Clayton JS (1966) Measurement of soil color. *Canadian Journal of Soil Science* 46, 83-90.

54 Smith T, Guild J. (1931) The C.I.E. colorimetric standards and their use. *Transactions of the Optical Society* 33, 73-134.

55 Sousa WP (1984) The role of disturbance in natural communities. *Annual Review of Ecology and Systematics* 15, 353-391.

56 Stenberg B, Viscarra Rossel RA, Mouazen AM, Wetterlind J (2010) Visible and near infrared spectroscopy in soil science. *Advances in Agronomy* 107, 163-125.

57 Stiglitz RY, Mikhailova EA, Post CJ, Schlautman MA, Sharp JL (2016) Teaching soil color determination using an inexpensive color sensor. *Natural Sciences Education* 45, 141-148.

58 Teye E, Huang X, Afoakwa N (2013) Review on the potential use of near infrared spectroscopy (NIRS) for the measurement of chemical residues in food. *American Journal of Food Science and Technology* 1, 1-8.

59 Thomaz EL (2018) Ash physical characteristics affects differently soil hydrology and erosion subprocesses. *Land Degradation and Development* 29, 690-700.

60 Úbeda X, Pereira P, Outeiro L, Martin DA (2009) Effects of fire temperature on the physical and chemical characteristics of the ash from two plots of cork oak (*Quercus suber*). *Land Degradation and Development* 20, 589-608.

61 Vergnoux A, Dupuy N, Guiliano M, Vennetier M, Theraulaz F, Doumenq P (2009) Fire impact on forest soils evaluated using near infrared spectroscopy and multivariate calibration. *Talanta* 80, 39-47.

62 Viscarra Rossel RA, Walvoort DJJ, McBratney AB, Janik LJ, Skjemstad JO (2006) Visible, near infrared, mid infrared or combined diffuse reflectance spectroscopy for simultaneous assessment of various soil properties. *Geoderma* 131, 59-75.

63 Wickham C (2018) munsell: utilities for using Munsell colours. R package version 0.5.0. https://CRAN.R-project.org/package=munsell